What are the benefits of lidar-assisted control in the design of a wind turbine?

Helena Canet[1], Stefan Loew[1], and Carlo L. Bottasso[1]

[1]Wind Energy Institute, Technical University of Munich, 85748 Garching b. München, Germany

Correspondence: Carlo L. Bottasso (carlo.bottasso@tum.de)

Abstract.

This paper explores the potential benefits brought by the integration of lidar-assisted control (LAC) in the design of a wind turbine. The study identifies which design drivers can be relaxed by LAC, and by how much these drivers should be reduced by LAC before other conditions become the drivers. A generic LAC load-reduction model is defined and used to redesign the

5 rotor and tower of three turbines, differing in terms of wind class, size and power rating. The load reductions enabled by LAC are used to save mass, increase hub height or extend lifetime. For the first two strategies, results suggest only modest reductions in the levelized cost of energy, with potentially benefits essentially limited to the sole tower of a large offshore machine. On the other hand, lifetime extension appears to be the most effective way of exploiting the effects of LAC.

1 Introduction

10 Wind turbines are highly dynamical systems, excited by stochastic and deterministic disturbances from wind. Among their various goals, wind turbine control systems try also to limit structural loads. In fact, lower ultimate and fatigue loading can be exploited by reducing mass and cost, or by designing larger and taller turbines that can generate more energy; in turn, all these effects may lead to a reduction of the cost of energy from wind.

Traditional wind turbine controllers rely on feedback measurements to drive blade pitch, generator torque and yaw. Since

15 they operate based on the response of the system as expressed by live measurements, these controllers are only capable of reacting to wind disturbances that have already impacted the wind turbine. This is an intrinsic limitation of all feedback-based mechanisms, which can only see the past but know nothing about the future. To improve on this situation, control systems can be augmented with preview information, which informs the controller on the wind that will affect the turbine in the immediate future.

20 Wind preview can be obtained from turbine-mounted *light detection and ranging* (lidar) sensors, which are capable of measuring various properties of the incoming flow field up to several hundred meters in front of the rotor. Lidar-augmented control strategies are generically termed lidar-assisted control (LAC).

Several lidar-enhanced control formulations have already been investigated, and their performance in terms of power capture and load mitigation are reported in the literature. Bossanyi et al. (2014) describe a feedback controller enhanced by a feedfor-

25 ward blade pitch loop enabled by lidar wind preview. Results indicate promising reductions in blade flap and tower fore-aft

fatigue damage, without any appreciable loss in power production. Similar benefits are also described by other sources as, for example, Dunne et al. (2011, 2012), and have been confirmed in the field (Schlipf et al., 2013c), albeit to the present date only on a small research wind turbine. Feedforward torque control strategies have also been investigated; results indicate marginal increments in mean power capture at the expense of high power and torque variations (Bossanyi et al., 2014; Wang et al., 2013; Schlipf et al., 2013). More advanced formulations, such as nonlinear model-predictive controllers (Schlipf et al., 2013b) or flatness-based controllers (Schlipf et al., 2014), have also been enhanced with lidar wind preview information. Promising results were reported in terms of load reductions and power increase, at the expense of a much higher computational cost, which makes real time execution more challenging to achieve and test in the field (Scholbrock et al., 2016).

Even though the potential of LAC is widely recognized, the system-level benefits that LAC may possibly bring to the levelized cost of energy (LCOE) are still not fully understood. In general two strategies have been suggested for reducing LCOE by LAC (Schlipf et al., 2018). The first is the *retrofit strategy*, which consists in using lidars to extend the lifetime of a wind turbine that has already been designed and installed. Schlipf et al. (2018) and Rubert et al. (2018) reported favorable results for towers, with lifetime extensions between 5 and 15 years. A second strategy is the *integrated approach*, in which LAC is considered as part of the system from its very inception. The idea in this second case is that, by considering LAC within the design process, its full potential can be realized by translating the benefits of load reductions directly into an improved turbine. Indeed, the adoption of a holistic system-level design approach was identified by IEA Task 32 on wind energy lidar systems (Simley et al., 2018) as an opportunity to assess the cost-benefit tradeoffs among turbine, lidar and control system.

This work aims at taking a small first step in this direction, providing an initial rough assessment of the potential benefits of considering LAC in the sizing of the two primary components of a wind turbine, namely the rotor and tower. The present work refines and expands the study described in Canet et al. (2020). In a nutshell, this study tries to give a preliminary answer to the following main research questions:

– To which extent can design-driving constraints be relaxed by LAC?

– What is the best way of reaping the benefits brought by LAC in the design of rotor and tower?

– To make LAC beneficial at the system-level, is it necessary to improve its performance or reduce its cost?

The presented investigation intentionally does not commit to a specific lidar hardware or control formulation. The effects of LAC are considered here through a load-reduction model, defined according to the average performance of LAC systems reported in the literature. To understand trends, rather than focusing on a specific case, a LAC performance range is defined by creating a pessimistic and an optimistic scenario from the average represented by the literature-sourced load-reduction model. Additionally, as design drivers are typically highly problem specific, the study is performed on three representative wind turbines, which differ for wind class, size and power rating.

The paper is organized as follows. Section 2 describes the approach and the models used in the study. First, the potential margins for improvement brought by LAC are analyzed. The idea here is to identify what would be the benefit of reducing some driving quantity, and by how much that quantity should be improved before another effect starts driving the design. Next,

a literature survey on LAC is used to define a load-reduction model. The section is concluded by a brief description of the cost models and of the design optimization procedures. Goal of the cost models is to identify the tradeoffs between weight savings made possible by LAC and the additional expenses due to the purchase and O&M costs of the lidar. Section 3 uses these methods and models to analyze the potential benefits of integrating LAC in the design of the tower and rotor of three different reference wind turbines. The study considers mass (and hence cost) reductions of the two components, but also investigates the design of towers that are taller or with a longer lifetime. The section is closed by a parametric analysis that looks at the effects of the purchase and maintenance costs of the on-board lidar system. Section 4 closes the paper by reporting and discussing the main conclusions of the study.

2 Approach

2.1 Assessment of potentially exploitable margins

Design-driving quantities can be affected by LAC only to some extent, past which some other effect beyond the reach of LAC becomes the driver, preventing further improvements. The extent by which a design driver can be affected by LAC is called here a *potentially exploitable margin* (PEM). It is an *exploitable margin* because, if it can be achieved, the design can be improved; it is however *potential* because it represents an upper bound and only a smaller improvement might be obtained by LAC than this maximum limit.

A PEM is clearly a very valuable piece of information: there is no point in using LAC to reduce a certain quantity past the value where the driver switches to some non-LAC controllable condition. In fact, any further reduction would be futile, as it would not affect the final design.

These considerations clearly do not apply exclusively to LAC, but more in general hold for any technology that has the potential to relax the design constraints of a system. Therefore, the analysis of PEMs is an extremely useful exercise, because:

– it is able to highlight the possible design benefits brought by the introduction of a new technology;

– it gives a target maximum margin of improvement that that technology should bring.

In the context of the current analysis, the assessment of PEMs is based on *key quantities* (ultimate and fatigue loads, elastic deflections), which result from the aeroservoelastic simulation of a comprehensive set of design load cases (DLCs) run with a non-LAC controller. DLCs represent the different operating conditions that a wind turbine encounters throughout its lifetime, as defined by certification standards (IEC, 2005).

For the purposes of this work, DLCs are classified in two distinct groups: *modifiable* and *blocking*. In modifiable DLCs, the maximum value of each key quantity depends on the controller. For example, this is the case for loads obtained in power production in normal turbulence conditions (DLC 1.X). In fact, by modifying the pitch-torque controller of the turbine, the response of the machine changes, and consequently the maximum loads that are produced also change. On the contrary, in blocking DLCs the key quantities are not affected by the controller. For instance, this is the case for loads generated in parked

conditions (DLC 6.X). In fact, as the pitch-torque controller is not active when the turbine is parked, it clearly cannot influence the loads that are generated in that condition. Table 1 presents a classification of the DLCs considered here, including a description of the corresponding operating condition.

Table 1. Classification of a selection of the design load cases into *modifiable* and *blocking* (see text for a definition). NTM = Normal turbulence model; ETM = Extreme turbulence model; ECD = Extreme coherent gust with direction change; EWS = Extreme wind shear; EOG = Extreme operating gust; EWM = Extreme wind speed model.

Classification	DLC	Design situation	Wind speed	Wind profile	Other condition
	1.1	Power production	$V_{\mathrm{in}}{:}V_{\mathrm{out}}$	NTM	
	1.2	Power production	$V_{\mathrm{in}}{:}V_{\mathrm{out}}$	NTM	
	1.3	Power production	$V_{\mathrm{in}}{:}V_{\mathrm{out}}$	ETM	
Modifiable	1.4	Power production	$V_{\mathrm{rated}} \pm 2$ m/s	ECD	
	1.5	Power production	$V_{\mathrm{in}}{:}V_{\mathrm{out}}$	EWS	
	2.1	Power production	$V_{\mathrm{in}}{:}V_{\mathrm{out}}$	NTM	Grid loss
	2.3 V_{o}	Power production	V_{out}	EOG	Grid loss
	2.3 V_{r}	Power production	$V_{\mathrm{rated}} \pm 2$ m/s	EOG	Grid loss
	6.1	Parked	V_{ref}	EWM 50 year	Yaw mis. ± 8 deg
Blocking	6.2	Parked	V_{ref}	EWM 50 year	Grid loss
	6.3	Parked	V_{ref}	EWM 1 year	Ext. yaw mis. ± 20 deg

PEMs are obtained via a two-step procedure.

First, the (active) design constraints that determine the sizing of a given wind turbine component are identified; these are termed *design drivers*. Design constraints are introduced in the structural design process of a wind turbine component to guarantee structural safety during its lifetime, ensuring that admissible values for stress, strain and fatigue damage are never exceeded. Additional constraints are enforced to avoid resonant conditions, to guarantee a safe clearance and avoid collisions between blade and tower, to prevent buckling, and to ensure all other desired characteristics from the resulting design (Bottasso and Bortolotti, 2019). These constraints are functions of the key quantities resulting from the various DLCs, augmented by safety factors as prescribed by the norms.

Second, all key quantities responsible for design-driving constraints are analysed, ranked in descending order, labelled with the indication of the originating DLC, and classified as modifiable or blocking. Clearly, the maximum value of a key quantity can only be reduced by LAC if its ranking is led by a modifiable DLC.

For each key quantity, its PEM is defined as the difference between its maximum value and the value of the highest ranked blocking DLC.

2.2 Estimation of benefits through structural redesign

Next, PEMs are exploited to improve the structural design of the wind turbine components that are not driven by blocking DLCs. To this end, DLCs should be run again, this time using a LAC controller to yield new values of the key quantities.

However, to make the analysis less specific to a given particular implementation, a LAC load-reduction model was used here
110 instead of re-running all DLCs with a given LAC controller in the loop. The load-reduction model is simply represented by
a coefficient smaller than one, defined for each key quantity associated with a modifiable DLC. The reduction coefficient is
based on results reported in the literature, as more precisely discussed in §2.2.1.

The application of a LAC load-reduction model lowers some of the key quantities, in turn deactivating the associated design-
driving constraints. To exploit the slack generated by LAC in the formerly active constraints, a redesign is performed to
115 determine the structure that minimizes a desired figure of merit while guaranteeing structural integrity, in turn reactivating the
constraints.

2.2.1 LAC load-reduction model

The load-reduction model is based on a literature survey. The study reported in Bossanyi et al. (2014) stands out, because
it provides a quantification of the effects of LAC on a rather comprehensive list of key quantities. That work used a simple
120 feedforward collective pitch LAC combined with a conventional feedback controller, applied to a 5 MW turbine. The paper
reports a significant reduction of damage equivalent loads (DELs) resulting from DLC 1.2 for blade, main bearing, tower top
and tower bottom. Extreme loads resulting from DLC 2.3 also experience significant benefits. On the other hand, power capture
—and hence Annual Energy Production (AEP)— is largely unaffected by this LAC implementation.

The load-reduction model derived from Bossanyi et al. (2014) is reported in Table 2 for each component and modifiable
125 DLC, in terms of percent changes with respect to a non-LAC controller. In the table, F and M respectively indicate force and
moment components, expressed in the (x, y, z) righthanded triad, where x points downstream, y is in the crossflow direction,
and z is vertical pointing upwards. Components not reported in the table experience either null or negligible reductions. For
simplicity, this model does not include lidar faults and assumes a lidar availability of 100%.

The load-reduction model of the table only includes DLC 1.1, 1.2, 1.3, and 2.3. In reality, these are not the only DLCs
130 that are modifiable —in the sense that they can be affected by a change in the controller—, and also DLC 1.4 (extreme wind
direction), 1.5 (extreme wind shear), and 2.1 (control system fault or grid disconnection) should be considered. The first two of
these DLCs are not considered in the LAC load-reduction model, because they do not typically generate design driving loads.
The case of DLC 2.1 is however different: here, maximum loads are typically generated during a shutdown, triggered by an
extreme ambient condition change, a fault or a grid disconnection. When this happens, the entity of the generated loads will be
135 largely dictated by the behavior of the shutdown procedure, which here is assumed not be assisted by a lidar for safety reasons.
On the other hand, loads generated during a shutdown might also depend to some extent on the state of the turbine at the time
the shutdown was triggered, which does depend on the behavior of the LAC controller. A precise quantification of the effects
of LAC on these DLCs would therefore require simulations with LAC in the loop, which are however outside of the scope
of the present preliminary work. Hence, LAC-induced load reductions were assumed to be null for these DLCs, which is a
140 conservative choice.

Clearly, differences in the formulation and tuning of a LAC controller will generally imply different reductions of key
quantities. To estimate these effects, the results obtained from various authors were compared. The most complete set of results

Table 2. Load-reduction coefficients based on Bossanyi et al. (2014), expressed as percentages with respect to a non-LAC controller.

	BLADE						
	Description	Fx	Fy	Fz	Mx	My	Mz
DLC 1.2	DEL	-3.8%	-0.1%	-0.25%	-0.4%	-3.8%	-3.5%
DLC 1.X	Extreme loads					-2.0%	
	Tip deflection					-2.0%	
DLC 2.3	Extreme loads					-2.9%	
	Tip deflection					-2.9%	
	MAIN BEARING						
	Description	Fx	Fy	Fz	Mx	My	Mz
DLC 1.2	DEL	-10.0%			-1.2%	-0.4%	-1.0%
DLC 1.X	Extreme loads						
	TOWER TOP (YAW BEARING)						
	Description	Fx	Fy	Fz	Mx	My	Mz
DLC 1.2	DEL	-12.0%	-0.1%	-2.1%	-2.0%	-1.8%	-0.2%
DLC 1.X	Extreme loads						
	TOWER BOTTOM						
	Description	Fx	Fy	Fz	Mx	My	Mz
DLC 1.2	DEL	-3.0%	0.2%	-2.2%	-0.1%	-12.0%	-0.2%
DLC 1.X	Extreme loads					-5.0%	
DLC 2.3	Extreme loads					-40.0%	

was found for DLC 1.2 in terms of DELs for fore-aft tower bending at tower top (FATBMTT), flapwise blade root moment (FBRM) and shaft torsional moment (STM), as reported by Schlipf et al. (2014); Bottasso et al. (2014); Haizmann et al. (2015);

145   Schlipf et al. (2015); Schlipf (2016); Sinner et al. (2018).

Table 3 reports the outcome of this analysis. There is a significant scatter in the results, especially for DEL FBRM and DEL STM, because of the variety of controller formulations and target wind turbine models. For instance, for DEL STM Schlipf et al. (2014) reports a load reduction of 30% using a flatness-based feedforward controller, while Schlipf (2016) reports an improvement of 6% when using a feedforward-feedback controller. The lower values reported in Bossanyi et al. (2014) are

150   most likely caused by the utilization of a fairly simple controller.

To address the conundrum posed by the scatter of the results reported in the literature, a pragmatic approach was used here. First, Bossanyi et al. (2014) was chosen as reference, because it presents a comprehensive list of effects on several components obtained by using a fairly plain implementation, which might be representative of an initial conservative deployment on production machines. Second, two additional sets of coefficients were added to the baseline ones of Bossanyi et al. (2014), to

155   represent *optimistic* and *pessimistic* scenarios. The optimistic scenario is obtained by multiplying the baseline coefficients by

Table 3. LAC-induced load reductions from Bossanyi et al. (2014) compared to other references.

	Bossanyi et al. (2014)	Additional literature
DEL FATBMTT	12	$(16.4 \pm 9.1)\%$
DEL FBRM	3.8	$(13.4 \pm 6.6)\%$
DEL STM	1.2	$(11.8 \pm 9.3)\%$

a factor of 1.5, whereas the pessimistic one is obtained by using a factor of 0.5. Here again, it is worth remembering that the present study does not target one specific LAC controller, but aims at understanding basic trends.

A distinction must be made between the application of load-reduction coefficients to ultimate loads and deflections, which is straightforward, and to fatigue loads. The former simply consists in the correction of the key quantities obtained by a non-LAC controller with the corresponding coefficients of the load-reduction model. Combined loads —for example at tower base or at the main and blade pitch bearings— are computed from the corrected individual load components.

For fatigue damage, the following procedure is used. Site-weighted DELs are computed as

$$\text{DEL} = \sum_{v=V_{\text{in}}}^{v=V_{\text{out}}} f(v) L_{eq}(v), \tag{1}$$

where $f(v)$ is the Weibull probability density function at a wind speed v, while the damage equivalent load at that same wind speed is expressed as

$$L_{eq} = \left(\frac{\sum_{i=1}^{n} S_{r,i}^{m}}{N_{eq}} \right)^{1/m}, \tag{2}$$

where m is the Wöhler coefficient, $S_{r,i}$ is the load range of a cycle i, n is the total number of cycles and N_{eq} the equivalent number of cycles (Hendriks and Bulder, 1995).

To compute LAC-reduced DELs, it is assumed that load reductions are independent of wind speed and load range. This way, the Weibull-weighted DEL reductions reported in the literature can be applied directly to the load time histories obtained here with a non-LAC controller by aeroelastic simulations. Next, transient combined loads are computed from the relevant components (for example, combining fore-aft and side-side components at tower base, and similarly combining the associated components at the main and pitch bearings), and then processed by rainflow counting to obtain DELs, finally searching for the point in the cross section of interest with the maximum damage.

2.3 Economic evaluation

During redesign, the components are evaluated from an economic point of view through suitable cost models, based on the characteristics of the wind turbine. The 2015 NREL cost model (WISDEM, 2020), which is an updated version of the 2006 model (Fingersh et al., 2006), is used for onshore machines, while the INNWIND cost model (Chaviaropoulos et al., 2014) is used for offshore turbines. The blade cost for both onshore and offshore models is computed based on the SANDIA model

180 (Griffith and Johans, 2013). All cost model outputs are expressed in 2020 Euros (€), inflated by the consumer price index and exchange rate. The comparison of the various designs is based on LCOE, which is computed as

$$\text{LCOE} = \frac{\text{FCR} \cdot \text{ICC}}{\text{AEP}} + \text{AOE,} \tag{3}$$

where FCR [-] is the Fixed Change Rate, ICC [€] the Initial Capital Cost, AEP [MWh] the Annual Energy Production, and AOE [€/MWh] the Annual Operating Expenses.

185 **2.4 Design and simulation environment**

Aeroelastic analyses are performed with the Blade Element Momentum (BEM) based aeroelastic simulator `Cp-Lambda` (Bottasso et al., 2016), coupled with a conventional non-LAC controller (Riboldi et al., 2012). The aeroelastic simulator `Cp-Lambda` is also the core of the wind turbine design suite `Cp-Max` (Bottasso and Bortolotti, 2019; Bortolotti et al., 2016). This code can perform the combined preliminary optimization of a wind turbine, including both rotor and tower sizing.

190   The optimization of the blade aeroelastic characteristics can be divided into two coupled sub-loops, which size the external aerodynamic shape and the structural components. In this work, the aerodynamic shape of the blade is kept frozen, and the rotor is redesigned only from the structural point of view.

    The blade structural optimization algorithm aims at minimizing cost, while guaranteeing structural integrity and other requirements by enforcing a set of constraints that include, among others, extreme conditions, fatigue damage, buckling, tower
195 clearance, frequency placement, manufacturability and transportation. The optimization variables include the thickness of the structural elements (skin, spar caps, shear webs) for given blade layout and materials. The inertial and structural characteristics of each blade section are computed with the 2D finite element cross-sectional analysis code `ANBA` (Giavotto et al., 1983).

    The tower structural sizing aims at minimizing tower cost, while satisfying constraints from extreme loads, buckling, fatigue damage, as well as geometric constraints for manufacturing and transportation. The optimization variables include the diameter
200 and thickness of the different tower segments for given material characteristics.

    The formal description of the design algorithms can be found in Bottasso et al. (2012) and Bortolotti et al. (2016). Optimization is based on Sequential Quadratic Programming (SQP), where gradients are computed by means of forward finite differences.

3 Results

205 The potential benefits of adopting LAC in the early stages of the design of the rotor and tower of different wind turbines are analyzed next, following the approach described in Section 2.

3.1 Reference machines

Three reference wind turbines are considered: WT1, an offshore class 1A (Bottasso et al., 2016); WT2, an onshore class 2A (Bortolotti et al., 2016); and WT3, an onshore class 3A (Bortolotti et al., 2019). The principal characteristics of these machines

210 are reported in Table 4, while additional details can be found in the corresponding references. These turbines are reasonable representatives of current products available on the market.

Table 4. Principal characteristics of the three reference turbines.

Turbine	WT1	WT2	WT3
IEC Class & Category	1A	2A	3A
Rated electrical power [MW]	10	2.2	3.4
Type	Offshore	Onshore	Onshore
Rotor diameter [m]	178.3	92.4	130.0
Specific power [W/m^2]	400.5	298.3	252.4
Hub height [m]	119.0	80.0	110.0
Blade mass [t]	42.5	8.6	16.4
Tower mass [t]	628	125	553

Table 5 compares the three machines in terms of capital cost (CAPEX), operational expenses (OPEX), AEP, and LCOE with some actual installations in the United States according to Stehly et al. (2017). The cost breakdown is expressed in 2017 United States Dollars (USD), and CAPEX does not include financial costs. The comparison shows a good match between the 215 costs of the onshore 2.2 MW WT2 turbine and the 2017 US land-based 2.32 MW machine. The costs of the 3.4 MW WT3 turbine, even if slightly higher for some figures, are also in reasonable agreement with the US reference. For the offshore case, a bottom-fixed 5 MW machine is compared to the 10 MW used in the present study. Larger differences are found here, for instance in the OPEX costs, due to the very different rating of the two turbines, although the LCOEs are relatively similar.

Table 5. Cost breakdown of the different reference models expressed in 2017 USD.

Cost [USD/kW]	Onshore			Offshore	
	Stehly et al. (2017)	WT2	WT3	Stehly et al. (2017)	WT1
Rating [MW]	2.32	2.2	3.4	5	10
CAPEX [USD/kW]	1454	1297	1759	3846	4379
OPEX [USD/kW]	43.6	48.1	51.4	144	225
AEP [MWh/MW]	3633	3520	3866	3741	4500
FCR [%]	7.9	7.9	7.9	7.0	7.0
LCOE [USD/MWh]	43.6	42.9	49.2	110.5	118.1

3.2 Assessment of potentially exploitable design margins

220 A reduced set of DLCs (IEC, 2005) is identified as the one producing design drivers for the three considered turbines. The set includes power production with normal turbulence (DLC 1.1), extreme turbulence (DLC 1.3), loss of electrical network in

normal turbulence (DLC 2.1) and with extreme operating gusts (DLC 2.3). Additionally, parked conditions are also considered in yaw misalignment (DLC 6.1), with grid loss (DLC 6.2) and with extreme yaw misalignment (DLC 6.3).

3.2.1 Tower

225   A first analysis of the loads and constraints driving the design of the three towers unveils a significant potential that could be exploited by LAC.

For the design constraint analysis, several cross-sections are considered along the tower height, where three local conditions are evaluated: buckling, ultimate strength based on von Mises stresses, and fatigue damage. Additionally, the placement of the first fore-aft and side-side frequencies is constrained to avoid crossing the one-per-rev at rated rotor speed.

230   For simplicity of discussion, only results at the tower top and bottom cross-sections are displayed in Fig. 1, where the constraint margins are displayed. These are formulated as the relative difference between the local conditions and their admissible values. A null value therefore indicates an active constraint, while a positive value indicates a slack condition, i.e. a constraint that is satisfied but inactive.
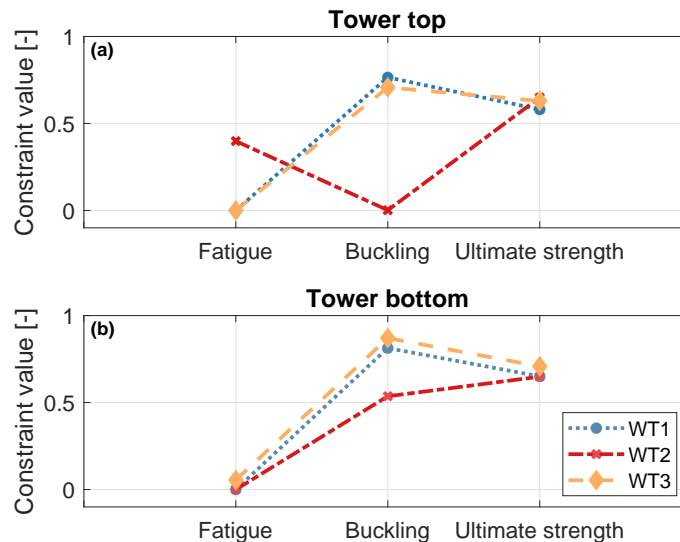
Figure 1. Design constraints at (a) tower top, and (b) tower bottom.

Considering first the tower top section, Fig. 1a shows that at this location the towers of WT1 and WT3 are driven by
235   fatigue, whereas buckling and strength are well below their maximum allowed values. The design of this section can therefore benefit from reductions in fatigue damage, which is mostly produced by the modifiable DLC 1.2 (power production in normal turbulence). On the other hand, the upper section of the WT2 tower is driven by buckling, whereas fatigue damage and ultimate strength are inactive. The PEM at this position along the tower is related to the combined bending moment (CBMTT). The rankings of this key quantity for the three turbines are shown in Fig. 2a. All values are normalized with respect to the leader

240 and, for clarity, only the leading and first blocking DLCs are shown. The ranking for WT2 is led by DLC 1.3, a modifiable DLC. The first blocking DLC is 2.1, which appears at position 28 in the ranking, leading to a PEM of about 20%.
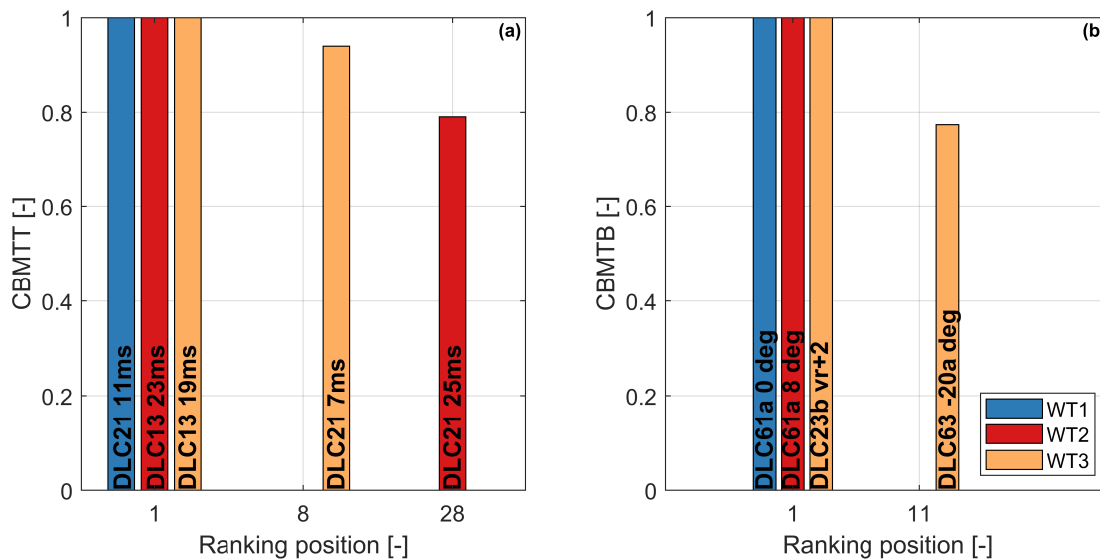
Figure 2. Ranking of normalized combined bending moment at (a) tower top (CBMTT) and (b) tower bottom (CBMTB), for the three turbines. Only the leading and first blocking DLCs are shown.

Considering the tower bottom cross section, Fig. 1b indicates that all three towers are driven by fatigue. Load rankings for combined bending moment at tower bottom (CBMTB) are reported in Fig. 2b. Results show no potential reduction for the extreme-load constraints, since the load rankings of the WT1 and WT2 towers are led by blocking DLCs. A margin of about 245 21% is visible for the WT3 tower, which however cannot be exploited since extreme loads do not drive the design at this section.

3.2.2 Rotor

Rotor design constraints include limits on the placement of the lowest natural frequencies to avoid resonant conditions, and a safe clearance with respect to the tower. Additionally, several cross sections are considered along the blade length, where upper 250 limits for strains, stresses and fatigue damage are prescribed on the spar caps, shell skin and shear webs. An excerpt from this extensive set of constraints is shown in Fig. 3; the skin, spar and web constraints are shown only at the midspan section of the blade, for simplicity of illustration.

The spar caps are the components that play the largest role in dictating the overall blade mass, as they mainly provide the blade flapwise bending stiffness. The design of these elements is driven by the blade-tower clearance constraint, which limits 255 the maximum blade tip displacement (Fig. 3a). On the other hand, stress, strain and fatigue constraints are all inactive (Fig. 3b). The tip displacement rankings, shown in Fig. 4a, indicate a significant reduction potential for all turbines, since they are all led
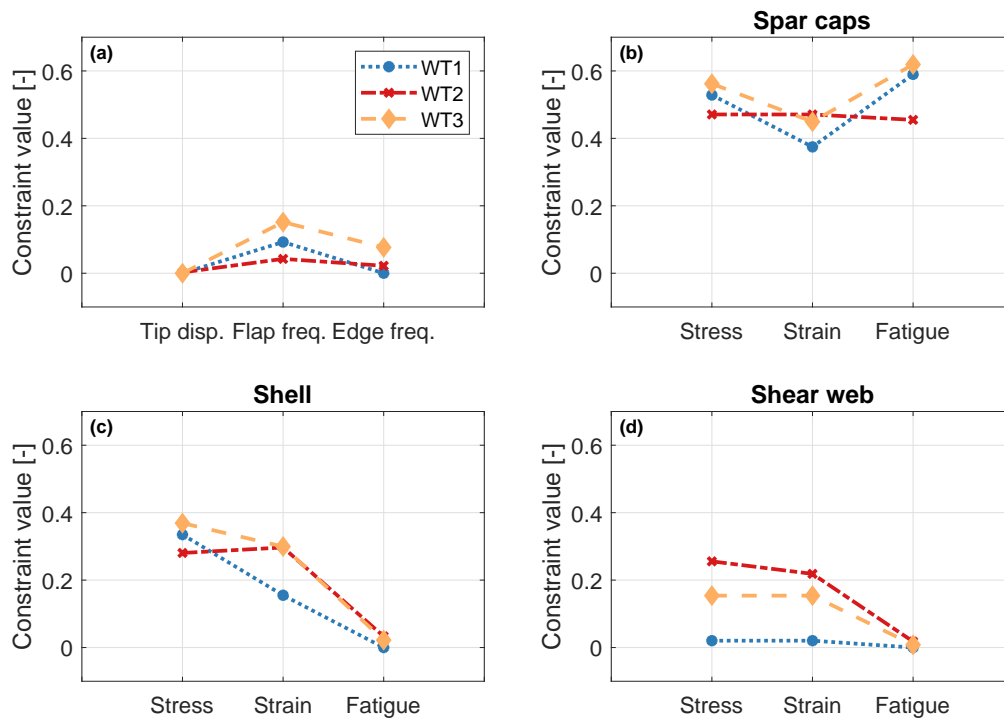
Figure 3. (a) Rotor design constraints. For a midspan section of the blade, design constraints at the spar caps (b), shell (c) and shear webs (d).

by modifiable DLCs. This key quantity for all three turbines is first blocked by DLC 2.1, leading to PEMs between 8% (WT1, ranking position 7) and 21% (WT2, ranking position 28).

The sizing of the shell skin is mainly driven by the fatigue damage constraint (Fig. 3c). This is also the main driver in the design of the webs, elements made of sandwich panels that carry shear. Fatigue damage is driven by the modifiable DLC 1.2. However, here the reduction potential is limited by technological constraints that bound from below the thickness of these elements. The load ranking of the combined blade root moment (CBRM) is shown in Fig. 4b, highlighting potential reductions. Indeed, all turbines are again first blocked by DLC 2.1, with large PEMs for WT2 (25%, ranking position 2) and WT3 (30%, ranking position 3).

3.3 Estimated benefits through structural redesign with LAC

This section aims at quantifying the benefits of integrating LAC within the design of the blade and tower of the three reference wind turbines. To this end, the rotor and tower of each turbine is reoptimized, considering loads and elastic deflections as reduced by the coefficients of the load-reduction model, using the factors of Table 2 and the optimistic (values incremented by 50%) and pessimistic (values reduced by 50%) scenarios. The economic evaluation is performed as indicated in Section 2.3,
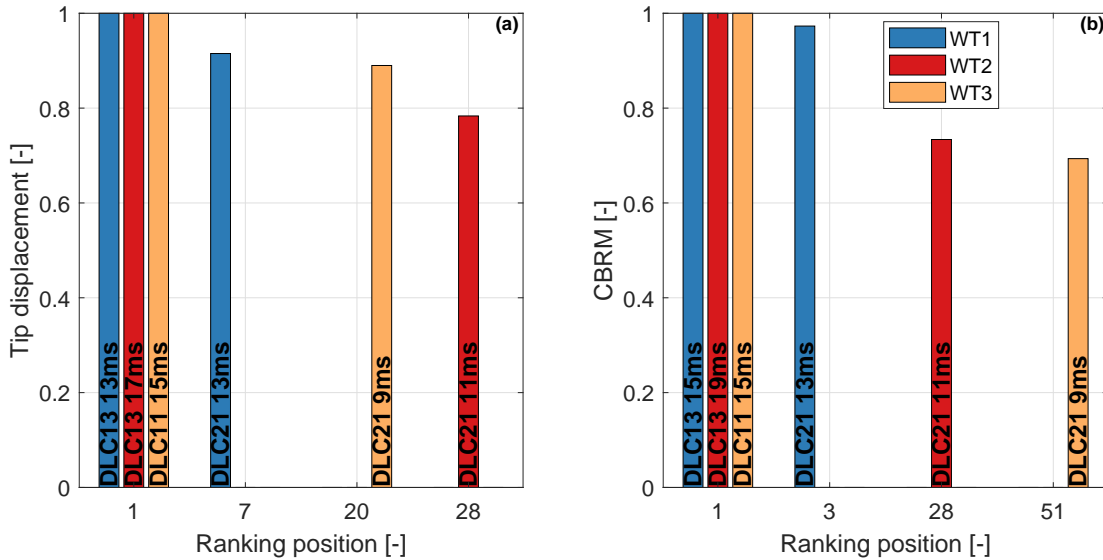
Figure 4. Ranking of (a) normalized blade tip displacement, and (b) combined blade root moment (CBRM), for the three turbines.

considering a fixed change rate (FCR) of 7%. It is further assumed that two lidar scanners have to be purchased over a turbine
lifetime of 20 years. This results in additional 100,000 € of ICC. Furthermore, the AOE includes an additional 2,500 €/year
of lidar O&M cost. These costs have been estimated based on input from two major lidar manufacturers, and only include
hardware-related costs. Due to a lack of information, the costs of development or licensing of LAC control software, related
commissioning and software maintenance have been neglected.

3.3.1 Tower redesign

Figure 5 reports changes in the LAC-based redesigned towers with respect to the initial baselines, when the tower height is held
fixed. The solid color bars correspond to the nominal load-reduction model, while whiskers indicate the effects of considering
the pessimistic and optimistic scenarios.

Both towers of WT1 and WT3 enjoy significant benefits from large reductions in fatigue damage, which decrease mass be-
tween 5% for the pessimistic scenario and 17% for the optimistic one. In turn, the lighter weight induces significant reductions
in the ICC of both turbines. On the other hand, the annual operating expenses (AOE) show a different behavior. Indeed, the
additional expenses generated by the maintenance of a lidar system do not significantly add to the already high O&M costs of
the offshore turbine WT1. For the onshore machines WT2 and WT3, where these costs play a larger role, AOE increases by
approximately 2%. For all turbines, AEP is essentially unaffected. In the end, the combination of these various effects produces
a reduction in LCOE of about 1.2% for WT1, and a very slight increase of 0.1% for this same figure of merit for WT3 (Fig. 5).

The WT2 tower presents a different trend. Indeed, the upper segment of this tower is driven by buckling. Even though this
constraint presents a significant PEM of about 20% (see Fig. 2a), LAC does not reduce extreme loads at tower top according
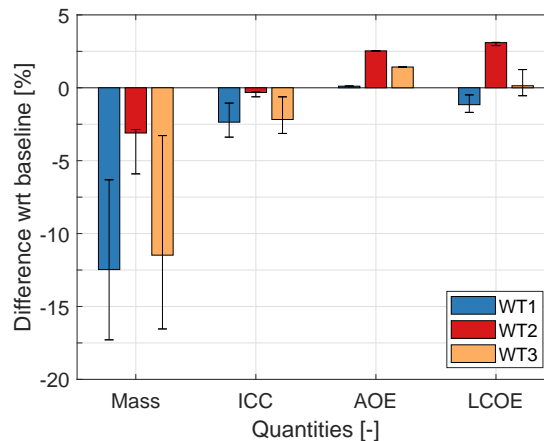
Figure 5. Effects of LAC on the redesign of the tower with respect to the initial baselines. Solid bars: load-reduction model of Table 2; whiskers: range of the pessimistic and optimistic scenarios.

to the load-reduction model (Table 2). As a consequence, the redesign is only capable of a limited mass reduction that, in combination with the significant lidar costs, leads to an increase in LCOE.

3.3.2 Taller tower redesign

Instead of reducing tower mass (and hence cost), LAC-based improvements in fatigue damage and ultimate loads can be exploited to design taller towers. In fact, by reaching higher above ground, the rotor is exposed to faster wind speeds, thus increasing AEP; thanks to LAC, this can be achieved without significantly increasing the cost of the tower. To explore the effects of this concept, towers of increasing heights were designed. The study assumes that LAC performance does not depend on tower height.

Here again the study is performed in two steps. First, the tower structure is sized with a non-LAC controller for a given height. The design objective is minimum mass, constrained to guarantee structural integrity. Next, the design is repeated by reducing the key quantities according to the load-reduction model, according to the nominal, pessimistic and optimistic scenarios. The procedure is repeated for increasing tower heights, until no further improvements are possible or an upper limit of 15% height increase with respect to the baseline is reached.

The effects on mass, ICC, AEP, AOE and LCOE for the three reference machines are reported in Fig. 6.

Different trends are observed for the three turbines. The offshore machine WT1 shows a larger potential: for each of the analyzed heights, mass reductions with respect to the non-LAC configuration always translate into decreases in ICC. At the same time AEP increases, whereas AOE remains mostly constant due to the already high O&M costs. LCOE decreases gradually as tower height is increased. However, most of the gains are already achieved for a height increase of 5%, which is associated with an LCOE decrease of about 1.5% (Fig. 6e).
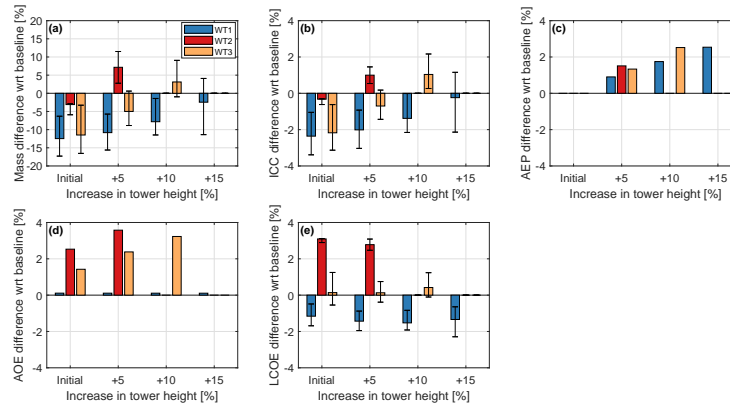
Figure 6. Effects of LAC on the redesign of towers of increasing height with respect to the initial non-LAC baselines. Solid bars: load-reduction model of Table 2; whiskers: range of the pessimistic and optimistic scenarios.

An opposite trend is obtained with the tower of WT2: because of its different design drivers, this machine does not benefit from a taller tower, as already noted in §3.2.1. The trend indicates that some LCOE improvements might be possible for very tall towers, which were however deemed unrealistic past the upper bound of a 15% height increase.

Similarly, a taller tower appears not to be very promising even for the onshore fatigue-driven WT3 turbine, although for different reasons. Here, although a 5% height increase lowers tower mass and ICC and improves AEP by about 2%, these benefits are offset by an increase in AOE, resulting in marginal —if not completely negligible— benefits in LCOE.

3.3.3 Tower redesign for longer lifetime

Instead of aiming for less expensive or taller towers, as done so far, yet another way to try and exploit the load benefits brought by LAC is to extend the tower lifetime.

In this case, the baseline towers are first designed for a 20 year lifetime based on the key quantities resulting from a non-LAC controller. Next, the towers are redesigned for increasing lifetime, based on key quantities modified by the load-reduction model. WT2 is excluded from this analysis, because of the very limited importance of fatigue in the sizing of its tower, as shown earlier.

The tower mass of both WT1 and WT3 increases substantially when sizing for a longer lifetime without using LAC. This negative effect is very nicely counteracted by the use of LAC. Figure 7 reports mass changes generated by LAC for increasing lifetime; all results are computed with respect to initial non-LAC 20-year baselines. At a lifetime of 40 years, which is double the conventional life duration, the tower mass of WT1 is still 10% lower than for the non-LAC 20-year case. The effect is similar, although a bit less pronounced, even for WT3: for a lifetime of 40 years with LAC, this tower has in fact nearly the same mass of the 20-year non-LAC design.
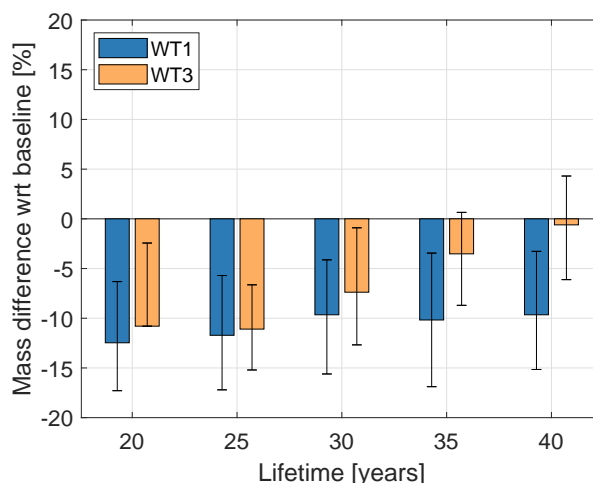
Figure 7. Effects of LAC on the redesign of towers of increasing lifetime with respect to 20-year non-LAC baselines. Solid bars: load-reduction model of Table 2; whiskers: range of the pessimistic and optimistic scenarios.

It should be remarked that these trends are obtained under the assumption of a 100% lidar availability; additionally, because of the approximations implicit in the assumed load-reduction model, these results can only be regarded as preliminary rough trends. However, the use of LAC to design towers with longer lifetimes seems to be much more promising than the alternative strategies of aiming for reduced costs or improved AEP by taller hub heights. Indeed, since the tower cost plays a large role in ICC, reductions in LCOE could be expected by the installation of towers with a longer lifetime. Alternatively, the towers could be reused to support more modern rotor-nacelle assemblies, playing the role of long term support structures that do not necessarily have to be upgraded at the same pace of the rest of the turbine.

3.3.4 Rotor redesign

Only rather modest mass reductions are achieved for the blades of all models and for all scenarios, due to the moderate influence of LAC in design-driving constraints. The situation is more precisely illustrated by Fig. 8, which shows the largest improvements for WT1 and essentially no effect for WT2.

Indeed, the load-reduction model reported in Table 2 shows a larger effect of LAC in fatigue damage mitigation than in the reduction of ultimate loads and deflections. Although webs and shear webs are both driven by fatigue, they are already thin structures with limited reduction potential before the thickness technological constraints become active. In turn, this leads to the fatigue PEMs not being fully exploited. The design of the spar caps is also not largely affected by LAC. In principle, a significant PEM is present for tip deflection, but unfortunately here again the LAC load-reduction model has only modest 2% improvements for this key quantity.
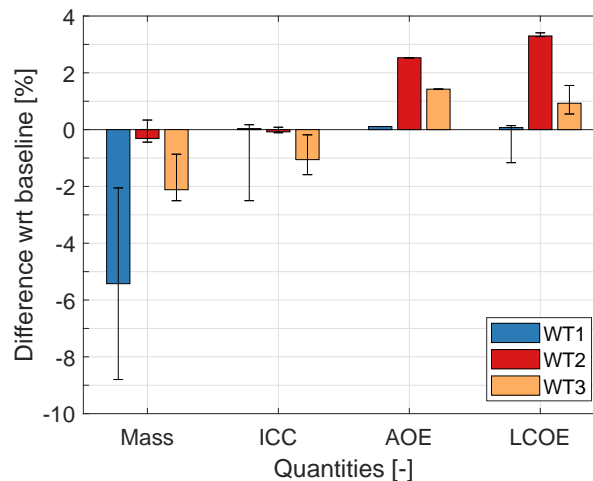
Figure 8. Effects of LAC on the redesign of the rotor with respect to the initial baselines. Solid bars: load-reduction model of Table 2; whiskers: range of the pessimistic and optimistic scenarios.

For all three turbines, the reduction in ICC generated by the use of LAC in the redesigned rotors is not significant enough to compensate for the increase in AOE. Therefore, LCOE increases for all onshore machines and decreases in a negligible way

345 for the offshore turbine.

3.4 Cost sensitivity analysis

Finally, a sensitivity analysis is performed to understand to what extent the purchase and maintenance costs of a lidar system can influence the reduction in LCOE. Baseline values of 100,000 € and 2,500 €/year, respectively for purchase and maintenance, are gradually modified until reaching the limit of ±100% variations. It is assumed that lidar-related yearly maintenance costs

350 are constant throughout the wind turbine lifetime, and are therefore not affected by external factors, such as the replacement of the lidar system. Purchase price includes both the cost and the number of lidar systems required throughout the wind turbine lifetime. The analysis considers the nominal LAC load-reduction model of Table 2 applied only to WT1 and WT3, as WT2 did not seem to have any real potential for improvement.

It should be noticed that purchase and maintenance costs are treated here as two independent variables. In reality, purchase

355 price could be correlated with performance, and therefore it might affect load reductions. Additionally, purchase price could be correlated with maintenance: a higher cost of the lidar could imply a more sophisticated device, which might be more costly to maintain, but it could also be correlated with build quality, which then might be inversely related to maintenance cost. Such considerations would require a sophisticated cost model of the lidar, which was however unfortunately not available for this research. The present analysis, being based on the simple change of the two independent quantities purchase and maintenance

360 costs, could then be interpreted as a price positioning study, where the lidar manufacturer tries to understand the correct price range for the device to make it appealing to customers.

Figure 9a shows that only a modest effect in LCOE can be achieved for WT1 when purchase and maintenance costs are modified. On the other hand, an order of magnitude larger effect is observed for WT3 (Fig. 9b), where the incidence of the lidar-associated costs is more prominent given the smaller size and rating of this turbine.

365 Break-even is indicated in both figures as a dotted line, located in the white area that separates reductions (blue) from increments (red) in LCOE. The break-even line is almost perpendicular to the purchase cost axis, implying a large sensitivity of LCOE to this quantity. The figure shows that reductions in purchase costs appear more effective than reductions in O&M costs. This seems to indicate that lidar manufacturers should try to keep the cost of the device as low as possible. The fact that maintenance costs are less relevant might indicate that simple and cheap lidars —although possibly a bit more expensive to
370 maintain— would be more appealing than sophisticated but expensive ones. Cheap single units, as long as availibility remains sufficiently high, might also be very interesting from the point of view of redundancy, which might open up the possibility of exploiting ultimate load reductions. However, as noticed earlier, more sophisticated models —capable of capturing the couplings among purchase price, performance (including availability), lifetime and maintenance— would be necessary to identify economically optimal development strategies for lidar systems.

375 Overall, results indicate that only modest reductions in LCOE are possible, even with very low LAC-induced costs.
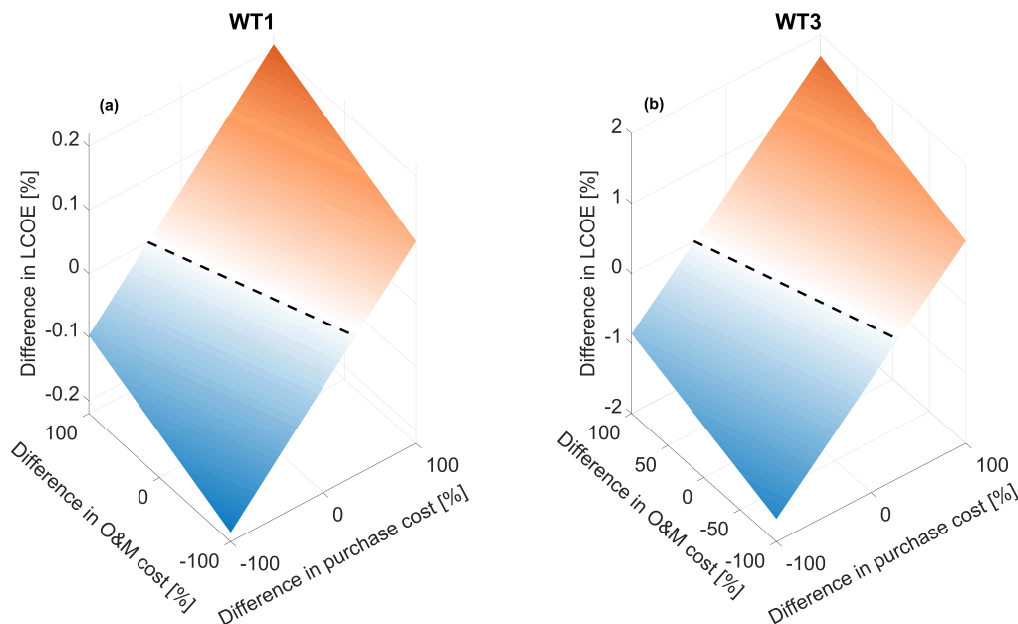
Figure 9. Percent variation of LCOE as a function of purchase and O&M costs of LAC systems for (a) the offshore machine WT1, and (b) the onshore machine WT3.

4   Conclusions

This paper has presented a preliminary analysis on the potential benefits of integrating LAC within the design of the rotor and tower of a wind turbine. The design was performed as a constrained optimization based on aeroelastic simulations, conducted in close accordance with international design standards.

380   The benefits generated by the use of a lidar in the control of a turbine were quantified through a load-reduction model derived from the literature, considering a variable performance of the LAC system within pessimistic and optimistic scenarios. This approach, in contrast to the use of an actual LAC controller in the loop, was chosen in order to draw conclusions on trends, rather than on the effects of a specific LAC controller and implementation. Realizing that any such redesign exercise is probably highly problem specific, the study was conducted considering three turbines of different class, size and rating.

385   Based on the results of this study, the following conclusions can be drawn.

First, a significant improvement potential was observed when the design is driven by fatigue. Indeed, fatigue damage is primarily generated in power production in turbulent wind conditions. Here, the lidar-generated preview of the wind that will shortly affect the rotor is clearly beneficial: as the controller "sees" what will happen, it can anticipate its action. This is in contrast to the case of a pure feedback controller that, since it can only operate in response to a phenomenon that has already

390   taken place, is by definition "late" in its reaction. In turn, the lidar preview information leads to a general reduction of load fluctuations, and hence of fatigue damage.

On the contrary, the improvement potential is only very limited for components driven by ultimate conditions (such as maximum stresses, strains or blade tip deflection). Indeed, these ultimate conditions cannot always be modified by LAC. In addition, even when LAC plays a role, other factors may have an even larger effect; for example, this is the case of shutdowns,

395   where the pitch-to-feather policy may have a dominant role in dictating the peak response. But even when LAC does relax a driving constraint, an even more general question still remains: shall one design a component based on a driver that was reduced by LAC? If so, what are the extra precautions that should be taken in order to hedge against faults, inaccuracies, misses, or unavailability of the lidar? These issues were not considered here, which is a limitation of the present study. However, it is possible that —at least in some of the cases analyzed in this work— the improvements to ultimate conditions brought by LAC

400   would have to be completely neglected when these additional aspects are considered, or that extra costs would have to be added, for example to ensure redundancy by the use of multiple lidars.

It was also found that, for fatigue-driven towers, significant benefits in mass can be obtained by the use of a LAC controller (on average by about 12% for the cases considered here). However, these benefits are largely diluted by looking at the more general metric LCOE. In fact, only a large offshore machine showed some improvements for this figure of merit: since O&M

405   costs are already high for an offshore turbine, the extra costs due to the lidar play a lesser role. For smaller turbines the situation is different, and the benefits in mass do not repay for the costs of the lidar.

Instead of simply reducing mass, LAC can be used to either increase hub height (which increases power capture in sheared inflow) or to extend lifetime. Both approaches were considered here. The most interesting results were again obtained for fatigue-driven offshore towers. Indeed, a 15% taller tower was found to present approximately the same mass of the baseline,

but with a 2% higher AEP. Even more interestingly, a LAC-enabled tower was designed with double the lifetime and 10% less mass than the baseline.

The situation for the rotor is less promising. In principle, spar caps —which are the main contributors to blade mass— could greatly benefit from LAC when tip deflection is the main driver. Here again lidar preview can clearly help when maximum deflections are triggered by strong wind gusts. On the other hand, stiffness requirements caused by the placement of the flap frequency can substantially reduce this margin of improvement, as this is a non-LAC modifiable effect. Additionally, one would have again to guarantee that the safety-critical tip clearance constraint is always satisfied during operation, which might require redundancy of the lidar or other measures. Webs and shell skin are often driven by fatigue, a condition that could in principle be exploited by LAC. However, the improvement potential is limited due to the already limited thickness of these components. In summary, the integration of LAC into the design of the rotor does not seem to lead to significant benefits in terms of LCOE.

Finally, a simple parametric study on the purchase and O&M costs of a lidar system was performed. As previously observed, the study shows that LCOE is largely independent from the LAC purchase and O&M costs in the offshore case. Although a larger effect is visible in the onshore case, improvements in LCOE caused by reductions in the lidars costs are still quite modest. This might indicate that, instead of targeting price reductions, lidar research and development should focus on performance. On the other hand, significant price reductions might allow for redundancy, which in turn would enable the targeting of ultimate conditions.

The present work is based on a number of assumptions, and further work should be performed before more definitive conclusions can be drawn. First, only three turbines were considered; although these machines are reasonable approximations of contemporary products, it is clear that design drivers are quite turbine specific, and a more ample range of cases should be investigated. Second, there was no attempt here to consider radar availability, faults and possible redundancy; an analysis of these aspects would help in clarifying whether ultimate conditions can indeed benefit from LAC or not. Finally, it should be remarked that the use of a generic load model implies some significant approximations. Although this was done here on purpose with the goal of making the study more general, it is also clear that the performance of different LAC systems can be very different, depending on the lidar characteristics and on the controller formulation and tuning. Therefore, here again, more specific studies could find niches of applicability of LAC missed by the present general analysis.

Notwithstanding the limitations of this study, in the end it appears that the answer whether LAC is beneficial or not might not be so clear cut, and in reality the situation is much more complex and varied (and also interesting). In hindsight, this is also a useful reminder that apparently obvious improvements do not always necessarily translate into real system-level benefits. For example, reducing some loads might be irrelevant if the design is driven by other factors, or might not pay off if the cost of that reduction neutralizes its benefits. This also stresses once more the central importance of systems engineering and design for the understanding of the true potential of a technology.

Author contributions. HC performed the analysis on potentially exploitable margins and conducted the design studies; SL prepared the lidar load-reduction model and assisted in the application of the model in the design framework; CLB formulated the analysis methodology based

on the new concept of potentially exploitable margins, proposed the use of a generic lidar load-reduction model, and supervised the work; HC and CLB wrote the paper. All authors provided important input to this research work through discussions, feedback and by improving

445   the manuscript.

Competing interests.   The authors declare that they have no conflicts of interest.

Acknowledgements.   The authors acknowledge the participants of the IEA Task 32+37 workshop "Optimizing Wind Turbines with Lidar-Assisted Control using Systems Engineering" for the valuable discussions.

References

450   Bortolotti P., Bottasso C.L. and Croce A.: Combined preliminary-detailed design of wind turbines, Wind Energ. Sci., 1, 71-88, https://doi.org/10.5194/wes-1-71-2016, 2016

Bortolotti P., Canet H., Dykes K., Merz K., Sethuraman L., Verelst D. and Zahle F.: IEA Wind TCP Task 37: Systems Engineering in Wind Energy — WP2.1 Reference Wind Turbines Technical Report, https://doi.org/10.2172/1529216, 2019

Bossanyi E., Kumar A. and Hugues-Salas O.: Wind turbine control applications of turbine-mounted lidar, J. Phys.: Conf. Ser., 555 012011,
455   https://doi.org/10.1088/1742-6596/555/1/012011, 2014

Bottasso C.L., Campagnolo F. and Croce A.: Multi-disciplinary constrained optimization of wind turbines, Multibody Syst. Dyn., 27, 21–53, https://doi.org/10.1007/s11044-011-9271-x, 2012

Bottasso C.L., Pizzinelli P., Riboldi C.E.D. and Tasca L.: LiDAR-enabled model predictive control of wind turbines with real-time capabilities, Ren. En., 71, 442–452, https://doi.org/10.1016/j.renene.2014.05.041, 2014

460   Bottasso C.L., Bortolotti P., Croce A. and Gualdoni F.: Integrated aero-structural optimization of wind turbines, Multibody Syst. Dyn., 38, 317–344, https://doi.org/10.1007/s11044-015-9488-1, 2016

Bottasso C.L., Bortolotti P.: Rotor Design and Analysis, Wind Energy Modeling and Simulation: Turbine and System, Veers P., Ed., ISBN 978-1785615238, The Institution of Engineering and Technology (IET), 2019

Canet H., Loew S. and Bottasso C.L.: Lidar-assisted control in wind turbine design: Where are the potential benefits?, J. Phys.: Conf. Ser.
465   1618 042020, https://doi.org/10.1088/1742-6596/1618/4/042020, 2020

Chaviaropoulos P., Karga I., Harkness C. and Hendriks B.: Deliverable 1.23 PI-Based assessment of innovative concepts *INNWIND.EU technical report*, www.innwind.eu, 2014

Dunne F., Pao L.Y., Wright A.D., Jonkman B. and Kelley N.: Adding feedforward blade pitch control to standard feedback controllers for load mitigation in wind turbines, Mechatronics, 21, 682–690, https://doi.org/10.1016/j.mechatronics.2011.02.011, 2011

470   Dunne F., Schlipf D, Pao L.Y., Wright A.D., Jonkman B., Kelley N. and Simley E.: Comparison of two independent lidar-based pitch control designs, Proc. AIAA Aerospace Sciences Meeting, Nashville, Tennessee, https://doi.org/10.2514/6.2012-1151, 2012

Fingersh L., Hand M. and Laxson A.: Wind Turbine Design Cost and Scaling Model, *National Renewable Energy Laboratory technical report* Golden, CO, NREL/TP-500-40566, 2006

Giavotto V., Borri M., Mantegazza P. and Ghiringhelli G.: Anisotropic beam theory and applications, Comput. Struct., 16, 403–13,
475   https://doi.org/10.1016/0045-7949(83)90179-7, 1983

Griffith D.T. and Johans W. 2013 Large blade manufacturing cost studies using the sandia blade manufacturing cost tool and Sandia 100-meter blades *Sandia National Laboratories technical report*, Albuquerque, NM SAND2013-2734, 2013

Haizmann F., Schlipf D., Raach S., Scholbrock A., Wright A., Slinger C., Medley J., Harris M., Bossanyi E. and Cheng P.W.: Optimization of a feed-forward controller using a CW-lidar system on the CART3, Proceedings of the American Control Conference, Chicago, USA,
480   https://doi.org/10.18419/opus-3975, 2015

Hendriks H.B. and Bulder B.H.: Fatigue Equivalent Load Cycle Method: A general method to compare the fatigue loading of different load spectrums, *Energy Research Centre of the Netherlands technical report*, Netherlands, ECN-C-95-074, 1995

International Electrotechnical Commission: International Electrotechnical Commission, IEC 61400-1 Ed.3: Wind turbines — Part 1: Design requirements, 2005

485 Riboldi C.E.D.: Advanced Control Laws for Variable-Speed Wind Turbines and Supporting Enabling Technologies, Ph.D. thesis (Politecnico di Milano), 2012

Rubert T., McMillan D. and Niewczas P.: A decision support tool to assist with lifetime extension of wind turbines, Renewable Energy, 120:423–433, 2018

Schlipf D., Fleming P., Kapp S., Scholbrock A., Haizmann F., Belen F., Wright A. and Cheng P.W.: Direct speed control using lidar and
490 turbine data, American Control Conference 2013, Washington DC, USA, https://doi.org/10.1109/ACC.2013.6580163, 2013

Schlipf D., Schlipf D.J., Kühn M.: Nonlinear model predictive control of wind turbines using lidar, Wind Energ., 16(7) 1107–1129, 2013

Schlipf D., Fleming P., Haizmann F., Scholbrock A., Hofsäß, M., Wright A. and Cheng P.W.: Field Testing of Feedforward Collective Pitch Control on the CART2 Using a Nacelle-Based Lidar Scanner, J. Physics 555 012090 10.1088/1742-6596/555/1/012090, 2013

Schlipf D., Cheng P.W.: Flatness-based Feedforward Control of Wind Turbines Using Lidar, IFAC Proceedings Volumes, Vol. 47, No. 3, pp.
495 5820–5825. https://doi.org/10.3182/20140824-6-ZA-1003.00443, 2014

Schlipf D., Simley E., Lemmer F., Pao L. and Cheng P.W.: Collective pitch feedforward control of floating wind turbines using lidar. Journal of Ocean and Wind Energy, 2(4), 2015

Schlipf D.: Lidar-Assited Control Concepts for Wind Turbines, Ph.D. Thesis (University of Stuttgart), 2016

Schlipf D., Fürst H., Raach S. and Haizmann F.: Systems Engineering for Lidar-Assisted Control: A Sequential Approach, J. Phys.: Conf.
500 Ser., 1102, 012014, https://doi.org/10.1088/1742-6596/1102/1/012014, 2018

Scholbrock A., Fleming P., Wright A., Wang N., Schlipf D. and Johnson K.: Lidar-Enhanced Wind Turbine Control: Past, Present and Future, NREL/CP-5000-65879, 2016

Simley E., Fürst H. and Schlipf D.: Optimizing Lidars for Wind Turbine Control Applications — Results from the IEA Wind Task 32 Workshop, Remote Sens., 10, 863, https://doi.org/10.3390/rs10060863, 2018

505 Sinner M.N. and Pao L.Y.: A Comparison of individual and collective pitch model predictive controllers for wind turbines, Annual American Control Conference (ACC), Milwaukee, WI, 2018, pp. 1509–1514, https://doi.org/10.23919/ACC.2018.8431598, 2018

Stehly T., Beiter P., Heimiller D. and Scott G.: Cost of Wind Energy Review, Tech. Rep. (National Renewable Energy Laboratory), https://www.nrel.gov/docs/fy18osti/72167, 2017

Wang N., Johnson K. and Wright A.: Comparison of strategies for enhancing energy capture and reducing loads using lidar and feedforward
510 control, IEEE Transactions on Control Systems Technology, 21, 1129–1142, https://doi.org/10.1109/TCST.2013.2258670, 2013

WISDEM Repository, https://github.com/WISDEM, 2020